Cuasi-coherent precursors and generation of filaments in the H-mode rotation layer

Florin Spineanu, Madalina Vlad, Daniela Nendrean

Association EURATOM-MEdC Romania

Vortex nucleation in strongly sheared velocity layers

Basic facts (in general supported by observations, still to be verified by experiments)

- in H mode a layer of plasma at the edge rotates poloidally with strong radial shear: this means a vorticity sheet
- there is a current sheet superposed on the vorticity sheet
- the current-vorticity sheet is unstable and breaks up into filaments

The mechanism of filamentation has the same nature as the instability of anomalous polytropic (Chaplygin) gases. The parallel dynamics is essential (is not collisional or Landau saturation).

Previous works: Ott, Trubnikov, Bulanov and Sasorov.

Vortex nucleation in protoplanetary accreation disks

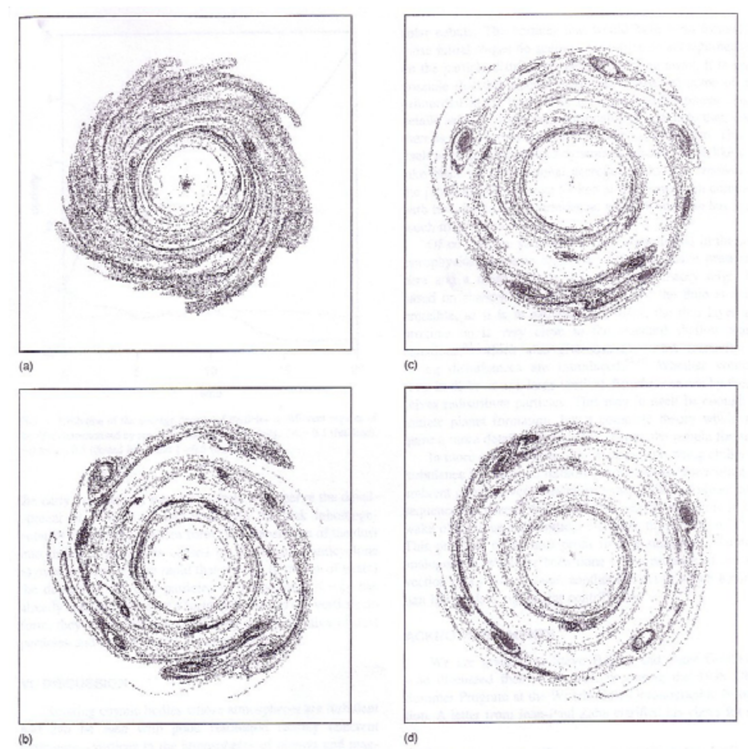

FIG. 3. (a) Distribution of the particles in the disk at time $t=2$ for $\gamma=10$; (b) Distribution of the particles at $t=8$; (c) Distribution of the particles at $t=15$; and (d) Distribution of the particles at $t=20$.

Vortex nucleation from unstable strongly sheared velocity layers
The case of the planetary atmosphere

2202 JOURNAL OF THE ATMOSPHERIC SCIENCES VOLUME 58

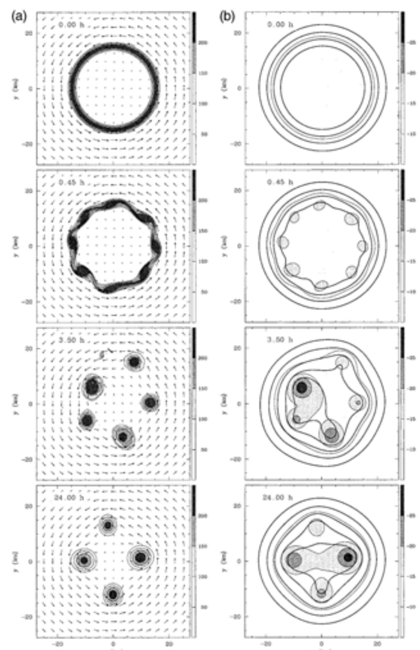

FIG. 4. (a) Vorticity contour plots and (u, v) wind vectors for expt. 1. The model domain is 200 km × 200 km but only the inner 55 km × 55 km is shown. The contours begin at $50 \times 10^{-4}\ s^{-1}$ and are incremented by $50 \times 10^{-4}\ s^{-1}$. Values along the label bar are in units of $10^{-4}\ s^{-1}$. Darker shading is associated with higher values of vorticity. (b) Pressure perturbation contour plots with contours of streamfunction (bold contours) superimposed. (Values along the label bar are in mb. Model run time in hours is shown on each plot.)

Non-neutral plasma: Breaking of a ring of vorticity into filaments

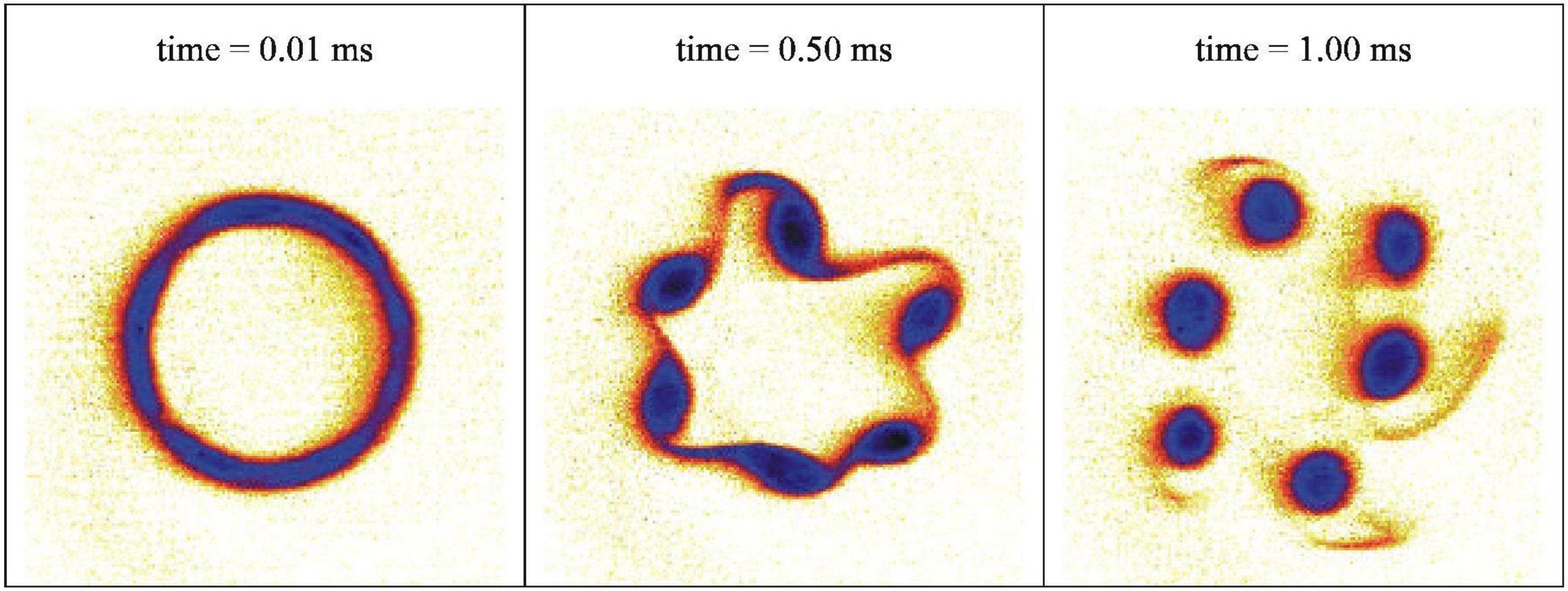

Figure 2.12: The Diocotron Instability.

Durkin, Schecter, Dubin, etc.

Stability of sheared layers

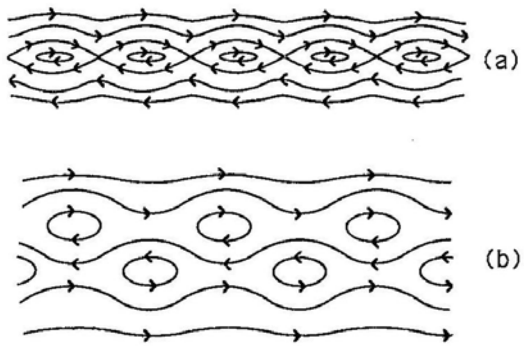

FIG. 1. Sketch of ideal streamfunctions, viewed from a reference frame moving with the structures. (a) Shear-induced vortex chain (Kelvin's "cat's eye"). (b) Rossby wave. The streamfunctions are plotted in the slab approximation, where curvature of the annulus is neglected.

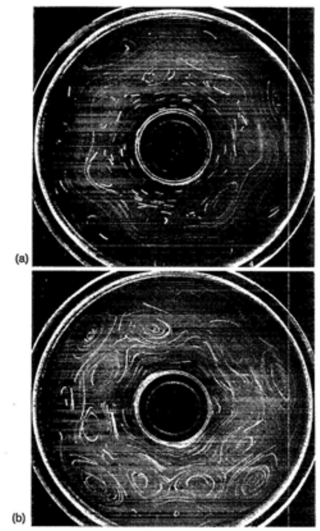

FIG. 18. Streak photographs of locked states: (a) corotating jet, (b) counter-rotating jet. In both cases there are seven vortices on each side of the jet, and the camera is in the comoving frame of the propagating vortices (exposure time = 8 sec, narrow forcing, $\nu = 0.033\ \mathrm{cm}^2/\mathrm{sec}$, $\Omega/2\pi = 1.50$ Hz, $F = 44.7\ \mathrm{cm}^3/\mathrm{sec}$).

Two kinds of perurbations:

cat's eye,

Rossby waves

Both these instabilities preserve the geometry of the flow.

Breaking of a sheared velocity layer into filaments of both signs

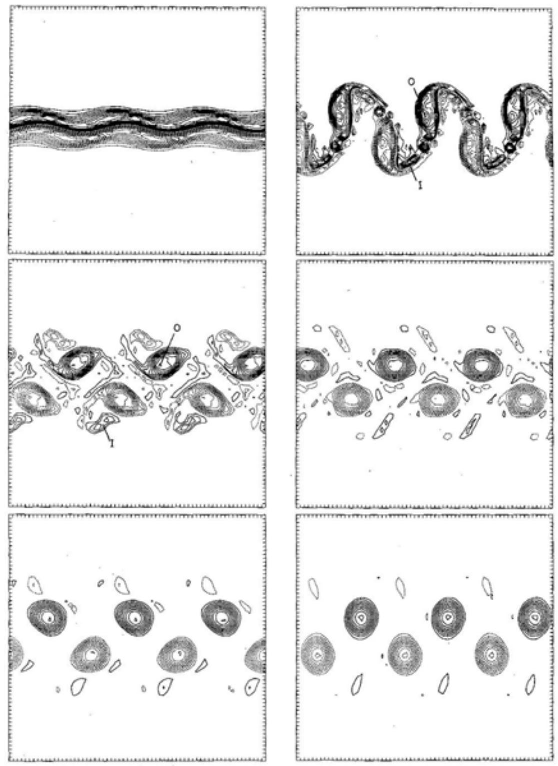

FIG. 3. Vorticity at $T = 16.6, 33.2, 49.8, 66.4, 83.0, 99.6$ for $k_0 = 0.736$ and $\beta = 0$. Arrows show outer and inner pools.

Flierl and Zabusky

There is a sort of current sheet at the edge superposed on the sheared velocity layer

056121-6 Burrell *et al.*

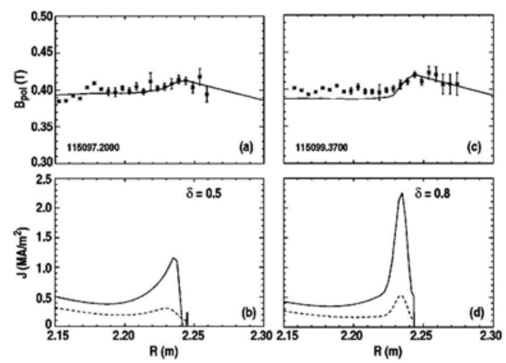

FIG. 9. Comparison of calculated poloidal magnetic field determined from the computed edge current density with the poloidal field measured by Zeeman polarization measurement from an injected lithium beam. (a) and (b) are for an upper single null discharge with triangularity 0.5 while (c) and (d) are for a balanced double null discharge with triangularity 0.8. The shapes are essentially identical to those shown in Fig. 7. In (b) and (d), the lower, dashed curve is the Ohmic plus bootstrap contribution to the overall current density while the upper, continuous curve is the total current density. Note that the current density is the local current density at the outer midplane of the plasma.

There is a current sheet superposed on the sheared layer

Breaking into localised structures of the density distribution in a layer of current

The width of the layer is initially L_0 and it evolves to a profile L which is variable along the direction y of the layer (poloidal).

Unperturbed state: $A = A_z(x) = -LB_0 \ln\cosh\left(\frac{x}{L}\right)$.

Using the notation

$$\rho(t,y) = \frac{nL(t,y)}{n_0 L_0}$$

we have the usual density conservation

$$\frac{\partial \rho}{\partial t} + \frac{\partial}{\partial y}(\rho v) = 0$$

The current density is

$$j_z = en(v_{iz} - v_{ez})$$

where

$$v_{iz} - v_{ez} = \frac{cB_0}{2\pi enL\left(t,y\right)} = \frac{\mathrm{const}}{nL}$$

The equation of motion is

$$\begin{aligned} \frac{\partial v}{\partial t} + v\frac{\partial v}{\partial y} &= \frac{1}{nm_i c}\left(-j_z B_x\right) \\ &= \frac{e}{m_i c}\left(v_{iz} - v_{ez}\right)\frac{\partial A}{\partial y} \end{aligned}$$

When the system is invariant along the z direction then the generalized momenta of the electrons and of ions are conserved

$$\begin{aligned} m_i v_{iz} + \frac{e}{c}A &= \mathrm{const} \\ m_e v_{ez} - \frac{e}{c}A &= \mathrm{const}' \end{aligned}$$

Then the equation of motion is

$$\frac{\partial v}{\partial t} + v\frac{\partial v}{\partial y} = \frac{e}{m_i c}\left(v_{iz} - v_{ez}\right)\frac{\partial A}{\partial y} = c_0^2 \frac{1}{\rho^3}\frac{\partial \rho}{\partial y} \tag{1}$$

The solution of the equations of the "Chaplygin" fluid

The two equations

$$\frac{\partial \rho}{\partial t} + \frac{\partial}{\partial y}\left(\rho v\right) = 0$$

and

$$\frac{\partial v}{\partial t} + v\frac{\partial v}{\partial y} = c_0^2 \frac{1}{\rho^3}\frac{\partial \rho}{\partial y}$$

is obtained using a *hodograph* transformation. The formulas are

$$\begin{aligned} \frac{nL}{n_0 L_0} &= \rho\left(t, y\right) = \frac{\sinh\left(|\tau|\right)}{\cosh\left(\tau\right) - \cos\chi} \\ \frac{v}{c_0} &= -\frac{\sin\chi}{\sinh\left(|\tau|\right)} \end{aligned}$$

where

$$\begin{aligned} \tau &= \frac{t}{t_*} < 0 \\ \chi &= \frac{x}{c_0 t_*} \end{aligned}$$

The *time*-like variable τ is introduced such that the unperturbed state is located at $t \to -\infty$ and the complete *breaking* of the layer is done when

$$\delta\chi = \pi \quad , \quad \text{at } \tau = 0$$

Solution showing breaking into singular structure

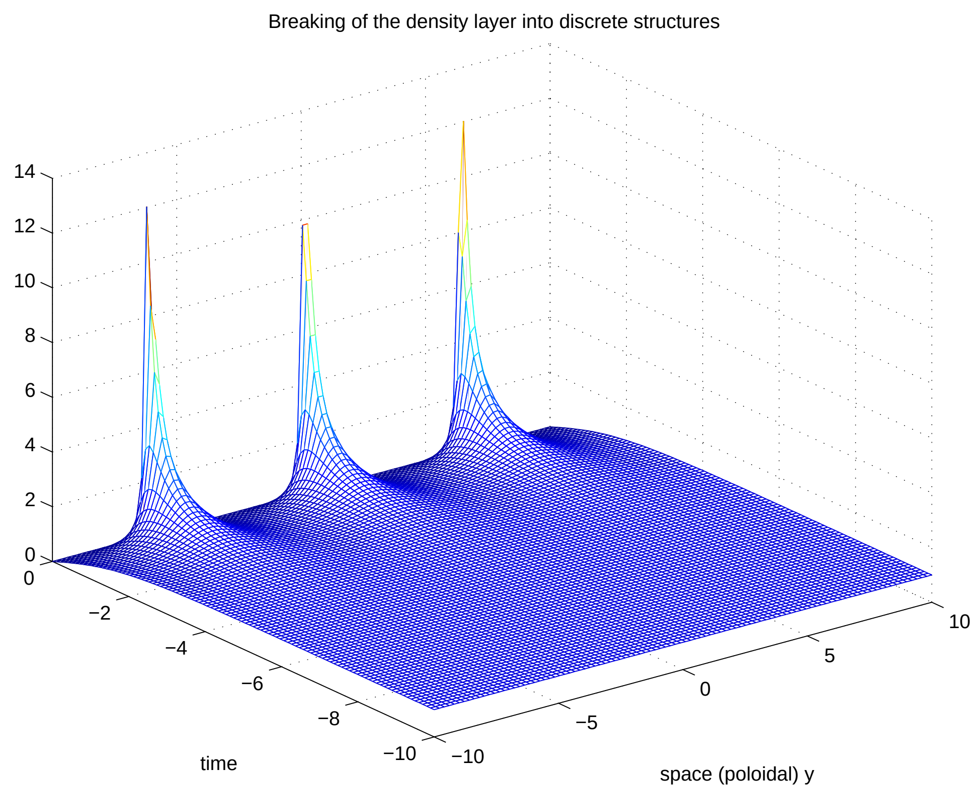

Tearing of the current layer

The equations are

$$\begin{aligned}
\frac{\partial v}{\partial t} + v\frac{\partial v}{\partial x} &= -\frac{e}{m_i c}\left(V_z^{(0)} + \frac{e}{m_e c}A\right)\frac{\partial A}{\partial x} \\
\frac{\partial n}{\partial t} + \frac{\partial}{\partial x}(nv) &= 0 \\
\frac{\partial^2 A}{\partial x^2} + \frac{\partial^2 A}{\partial y^2} &= \frac{4\pi e L}{c}\delta(y)\, n\left(V_z^{(0)} + \frac{e}{m_e c}A\right)
\end{aligned}$$

where

$$V_z^{(0)} \equiv v_{ez}^{(0)} - v_{iz}^{(0)}$$

This solution is

$$\begin{aligned} \pm\frac{y}{c_0 t_*} &= \chi(\tau,\rho) \\ &= \lambda + \arctan\left(\frac{\lambda}{|\tau|}\right) \end{aligned}$$

and

$$\lambda = \sqrt{\frac{|\tau|\,\rho}{1-\rho} - \tau^2}$$

where

$$\begin{aligned} \rho &< 1 \\ -\infty &< \lambda < +\infty \end{aligned}$$

The solution representing a single hill

This is of the form

$$\begin{aligned}\pm\frac{y}{c_0 t_*} &= \chi(\tau,\rho) \\ &= \pi+\lambda-\arctan\left(\frac{\lambda}{|\tau|}\right)\end{aligned}$$

and

$$\lambda=\sqrt{\frac{|\tau|\,\rho}{\rho-1}-\tau^2}$$

The quickest growing solution is the periodic one

$$\begin{aligned}\pm\frac{y}{c_0 t_*} &= \chi(\tau,\rho)=z+\arctan\left(\frac{z}{r-1}\right) \\ z &= \sqrt{\exp(-\tau/2)-\left(\frac{1}{\rho}-1\right)^2}\end{aligned}$$

The density varies between the limits

$$\frac{1}{1+\exp\left(-\left|\tau\right|\right)} = \rho_{\min} < \rho < \frac{1}{1-\exp\left(-\left|\tau\right|\right)}$$

The solution describes periodic hills whose maxima become infinite at

$$\tau \to -0$$

but the minima are never exactly 0.

The solution from Troubnikov

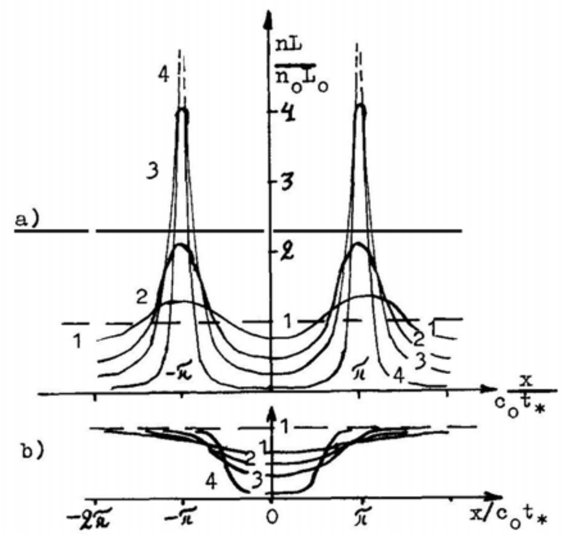

Fig. 12. Tearing of the plasma density (nL/n_0L_0) – periodic in "x" (a) and localized (b) – in a thin neutral current-carrying layer. Curves 1–4 correspond to the parameter $\gamma t = -2, -1, -0.5, -0.1$.

There is a breaking up of the density in the layer

The density is higher on both sides of the maxima of vorticity.

Conclusions

A layer of plasma where there is vorticity concentration (sheared poloidal rotation) is also an attractor for current density concentration (three reasons: trivial equilibrium in a high pressure gradient pedestal; higher bootstrap current, due to high pressure gradient; and MHD optimal equilibria). This layer is unstable to separation into distinct highly concentrated regions which at the limit may become cuasi-singular. The reason of this filamentation is basically the three dimensional dynamics constrained by the conservation of the parallel invariant. It turns the balance equations into those of a gas with anomalous polytropic, like Chaplygin gas.

How is flow at the edge

ALCATOR C

things are evident. First, the velocities inside the separatrix (on the closed flux surfaces) are essentially purely poloidal and point downward. This is in the ion diamagnetic direction and corresponds to a positive E_r if the perturbation movement is dominated by $E_r \times B$ motion. Magnitudes are of order 500 m/s. Second, at the separatrix the velocities change direction abruptly. In this case the motion in the SOL is predominantly radially outward, with 500 m/s as the order of magnitude. Third, in the SOL there is a radial acceleration.

This is in Alcator C mode

Left: Observed filaments in MAST

Right: supposed filaments in MAST

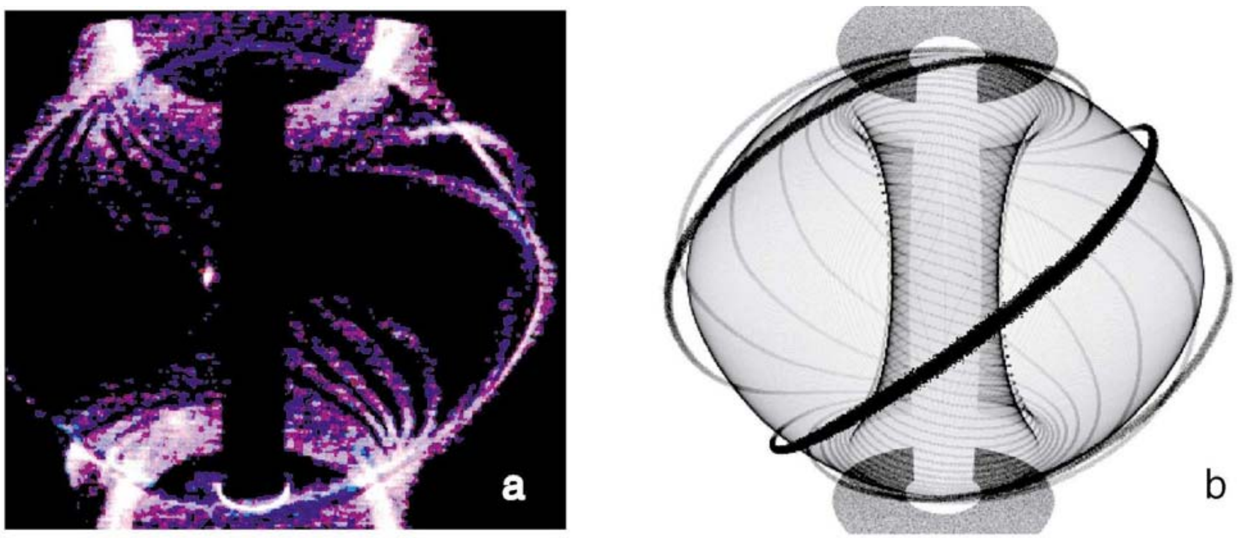

FIG. 4 (color). (a) High-speed video image of the MAST plasma obtained at the start of an ELM. (b) The predicted structure of an ELM in the MAST tokamak plasma geometry, based on the nonlinear ballooning mode theory.

MAST, Kirk 2005

The idea about filaments in MAST

The following is a possible interpretation of the experimental observations. During the inter-ELM period, steep gradients in both density and temperature develop just inside the separatrix in the pedestal region, reaching a peak shortly before the ELM [Fig. 2(a) shows a typical density profile]. At this time, the axisymmetric magnetic geometry is unperturbed [Fig. 2(d)]. At the onset of the ELM, narrow plasma filaments develop, locally perturbing the outboard separatrix and flux surfaces in the scrape-off layer [Fig. 2(e)]. Although these are extended along a field line, the perturbations appear to be poloidally localized at any particular toroidal angle. Thomson

MAST, Kirk 2005

From ALCATOR C mode

is ballooning-like. One of its common characteristics is the generation of 'filaments' of the density and potential perturbations that are field-aligned and have small $k_{\|}$.

Observations on intermittent transport

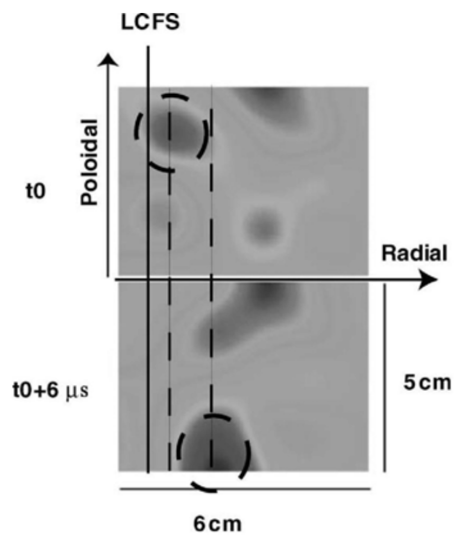

Fig. 4. Two frames from BES showing 2-D density plots. There is a time difference of 6 μs between frames. A particular structure is marked with a dashed circle, and shown in both frames, clearly highlighting poloidal and radial motion.

The idea about the intermittent structures

SOL) and the abscissa to time. The data, which is not shown in the same scale for clarity, displays structures that appear intermittently, travel radially and poloidally and then dissipate. Notice that the structures are born in a region (marked with a dashed line) slightly inside the LCFS (marked with a solid line) *only and do not come from deeper in the plasma core.* The intensity of the in-

The tearing of the density distribution in a layer of current

The current sheets are unstable to the tearing instability and they can be torn apart into strips of current.

The width is initially L_0 and it evolves to a profile L which is variable along the direction y of the layer (poloidal). The magnetic field has a shear

$$B = B_y(x) = -B_0 \tanh\left(\frac{x}{L}\right)$$

and we introduce the z component of the magnetic potential

$$B_y = \frac{\partial A}{\partial x}$$

$$A = A_z(x) = -LB_0 \ln\cosh\left(\frac{x}{L}\right)$$

in the unperturbed state. The magnetic field has the magnitude B_0 at the upper and lower limits of the layer (with opposite directions).

The process consists of the deformation of the profile of the leyer

$$L_0 \to L(t, y)$$

In the layer there is the current and on every unit length of the layer along x the **total** current is

$$i_z^0$$

When the layer thickness on x is smaller than the ion Larmor radius, the magnetic field *can penetrate* the deformed surface of the layer. In the *long wave* limit the magnetic field at the surfaces of the deformed layer

$$x = \pm \frac{L(t, y)}{2}$$

does not differ too much of B_0. Then the **total** current per unit of

y-length is always the same

$$\begin{aligned} i_z &= L(t,y)\, j_z \\ &= i_z^0 = \frac{cB_0}{2\pi} \end{aligned}$$

The current density is

$$j_z = en\left(v_{iz} - v_{ez}\right)$$

(here $e = |e|$). The plasma is neutral

$$n_e = n_i = n$$

Then

$$v_{iz} - v_{ez} = \frac{cB_0}{2\pi enL(t,y)} = \frac{\text{const}}{nL}$$

We note that the product

$$nL$$

is actually a density of the plasma (on every unit y-length). We have to keep the conserved number of particles

$$\frac{\partial}{\partial t}(nL) + \frac{\partial}{\partial y}(vnL) = 0$$

where v is the velocity of plasma along the direction of the layer, y. One can introduce a normalized density of plasma

$$\rho(t,y) = \frac{nL(t,y)}{n_0 L_0}$$

and the previous equation becomes the usual density conservation

$$\frac{\partial \rho}{\partial t} + \frac{\partial}{\partial y}(\rho v) = 0$$

In the equation of motion only the $\mathbf{j} \times \mathbf{B}$ term is important

$$\begin{aligned}
\frac{\partial v}{\partial t} + v\frac{\partial v}{\partial y} &= \frac{1}{nm_i c}\left(-j_z B_x\right) \\
&= \frac{e}{m_i c}\left(v_{iz} - v_{ez}\right)\frac{\partial A}{\partial y}
\end{aligned}$$

When the system is invariant along the z direction then the generalized momenta of the electrons and of ions are conserved

$$\begin{aligned}
m_i v_{iz} + \frac{e}{c}A &= \text{const} \\
m_e v_{ez} - \frac{e}{c}A &= \text{const}'
\end{aligned}$$

Then

$$\frac{\partial A}{\partial y} = -\frac{c m_i m_e}{e\left(m_e + m_i\right)}\frac{\partial}{\partial y}\left(v_{iz} - v_{ez}\right)$$

The difference of the two velocities is obtained from the continuity equation, expressed in terms of the quanity nL,

$$\begin{aligned} v_{iz} - v_{ez} &= \frac{cB_0}{2\pi} \frac{1}{nL} \\ &= \frac{cB_0}{2\pi n_0 L_0} \frac{1}{\rho} \end{aligned}$$

from which we get

$$\frac{\partial}{\partial y} (v_{iz} - v_{ez}) = \frac{cB_0}{2\pi n_0 L_0} \left(-\frac{1}{\rho^2} \frac{\partial \rho}{\partial y} \right)$$

The equation of motion is

$$\begin{aligned} \frac{\partial v}{\partial t} + v \frac{\partial v}{\partial y} &= \frac{e}{m_i c} (v_{iz} - v_{ez}) \frac{\partial A}{\partial y} \\ &= c_0^2 \frac{1}{\rho^3} \frac{\partial \rho}{\partial y} \end{aligned}$$

The constant is

$$c_0 = \frac{2v_A \delta_0}{L_0}$$

The other condition is

$$\delta_0 \ll L_0$$

The solution of the equations of the "Chaplygin" fluid

The two equations

$$\frac{\partial \rho}{\partial t} + \frac{\partial}{\partial y}(\rho v) = 0$$

and

$$\frac{\partial v}{\partial t} + v\frac{\partial v}{\partial y} = c_0^2 \frac{1}{\rho^3}\frac{\partial \rho}{\partial y}$$

is obtained using a *hodograph* transformation. The formulas are

$$\begin{aligned} \frac{nL}{n_0 L_0} &= \rho(t,y) = \frac{\sinh(|\tau|)}{\cosh(\tau) - \cos\chi} \\ \frac{v}{c_0} &= -\frac{\sin\chi}{\sinh(|\tau|)} \end{aligned}$$

where

$$\begin{aligned} \tau &= \frac{t}{t_*} < 0 \\ \chi &= \frac{x}{c_0 t_*} \end{aligned}$$

The *time*-like variable τ is introduced such that the unperturbed state is located at $t \to -\infty$ and the complete *tearing* of the layer is done when

$$\delta\chi = \pi \quad , \quad \text{at } \tau = 0$$

The solution is obtained indirectly; first

$$y\,(t,\rho)$$

The solution of tearing This solution is

$$\begin{aligned} \pm\frac{y}{c_0 t_*} &= \chi\,(\tau,\rho) \\ &= \lambda + \arctan\left(\frac{\lambda}{|\tau|}\right) \end{aligned}$$

and

$$\lambda = \sqrt{\frac{|\tau|\,\rho}{1-\rho} - \tau^2}$$

where

$$\begin{aligned} \rho &< 1 \\ -\infty &< \lambda < +\infty \end{aligned}$$

The solution representing a single hill This is of the form

$$\begin{aligned} \pm\frac{y}{c_0 t_*} &= \chi(\tau,\rho) \\ &= \pi + \lambda - \arctan\left(\frac{\lambda}{|\tau|}\right) \end{aligned}$$

and

$$\lambda = \sqrt{\frac{|\tau|\,\rho}{\rho-1} - \tau^2}$$

The quickest growing solution is the periodic one

$$\begin{aligned} \pm\frac{y}{c_0 t_*} &= \chi(\tau,\rho) = z + \arctan\left(\frac{z}{r-1}\right) \\ z &= \sqrt{\exp(-\tau/2) - \left(\frac{1}{\rho} - 1\right)^2} \end{aligned}$$

The density varies between the limits

$$\frac{1}{1+\exp\left(-\left|\tau\right|\right)} = \rho_{\min} < \rho < \frac{1}{1-\exp\left(-\left|\tau\right|\right)}$$

The solution describes periodic hills whose maxima become infinite at

$$\tau \rightarrow -0$$

but the minima are never exactly 0.

The solution from Troubnikov

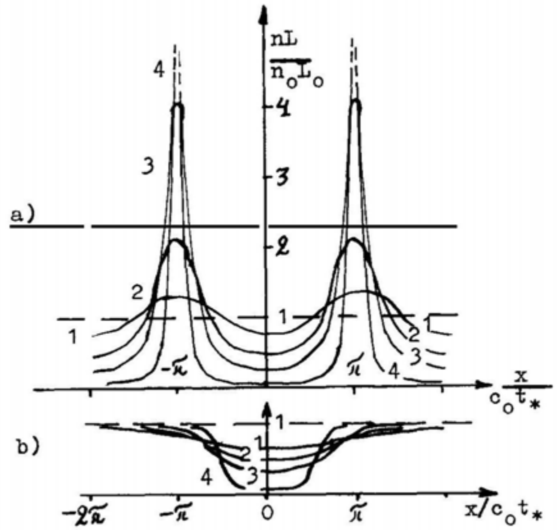

Fig. 12. Tearing of the plasma density (nL/n_0L_0) – periodic in "x" (a) and localized (b) – in a thin neutral current-carrying layer. Curves 1–4 correspond to the parameter $\gamma t = -2, -1, -0.5, -0.1$.

There is a breaking up of the density in the layer

The density is higher on both sides of the maxima of vorticity.

Vortex nucleation is superfluids and in Bose-Einstein condensates

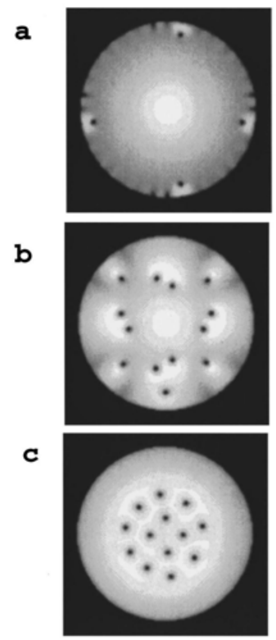

FIG. 3. The sequence of grey-coded images of $|\Psi|$ demonstrating nucleation of vortices and creation of the vortex lattice. The dark shade corresponds to zero of $|\Psi|$; the white one to its maximum value. Vortices are seen as black dots. The parameters are $\Omega = 0.01$, $R = 65$, $\Lambda \gg 1$. The initial condition is $\Psi = 1$ plus small-amplitude broadband noise. (a) $t = 100\Lambda$, (b) $t = 200\Lambda$, (c) $t = 1100\Lambda$.

The condition of creation of a vortex *ring* has been formulated by Feynman :

the velocity of the superfluid component must be greater than the *velocity self-induced by the ring*

$$V_{sf} > V^{ring} = \frac{\hbar}{2mR} \ln\left(\frac{8R}{a} - 1\right)$$

and the self-energy of the flow in a vortex ring is

$$E^{ring} = \rho_s \frac{\hbar^2 \pi^2}{m^2 R} \left[\ln\left(\frac{8R}{a}\right) - 3\right]$$

This energy is taken by **Langer Fischer** at the exponent of a barrier-type expression for the probability of nucleation

$$\Gamma = \Gamma_0 \exp\left(-\frac{E^{ring}}{kT}\right)$$

The Kelvin-Helmholtz instability actually breaks up he flow into separated filaments that evolve to produce a single vortex.
Destruction of a sheared layer: generation of vortices followed by vortex merging

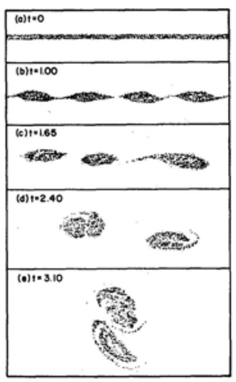

FIG. 1. The evolution of coherent vortices in a free shear layer perturbed by white noise: (a) the initial shear layer, (b) the first instability stage, (c) a local pairing between the right two vortices, (d) a subsequent pairing between vortices on the left, and (e) a pairing of the two larger vortices.

Moon Weidman, Local Vortex Pairing
3805 Phys. Fluids, Vol. 31, No. 12, December 1988

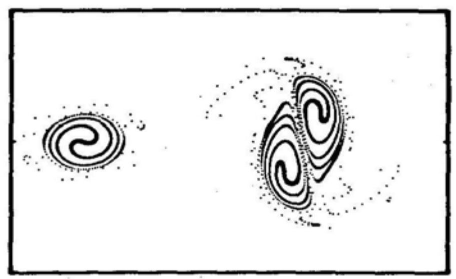

Moon Wei
Local Vort
PF31 (198

FIG. 3. Secondary instability of the vortices when the shear lay
by mode $k_0/3$ with relative phase $\theta = -\pi/3$ [cf. Eq. (3)].

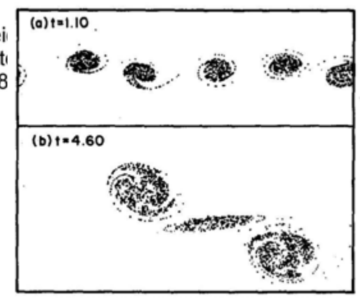

Moon Weidman
Local Vortex Pairing
PF31 (1988) 3804

FIG. 4. The evolution of vortices in an unforced shear layer when the box size is increased to contain five natural vortices. (a) Flow development shortly after the first instability stage and (b) a later picture showing two paired vortices and a "dropout."

KH instability when there is a weak magnetic field

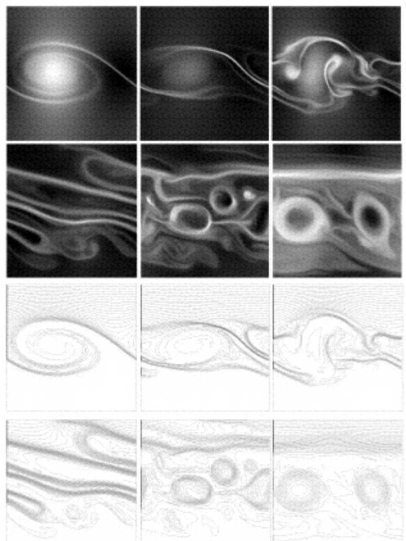

If the magnetic field parallel to v is small

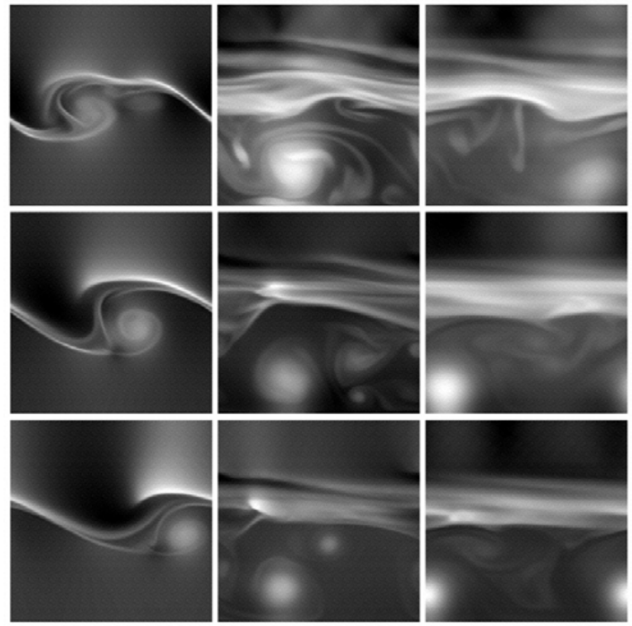

Typical for ionosphere

However for fields like in tokamak the KH instability is either suppressed or it has small growth rate.

KH : There is a magnetic field perpendicular on the plane

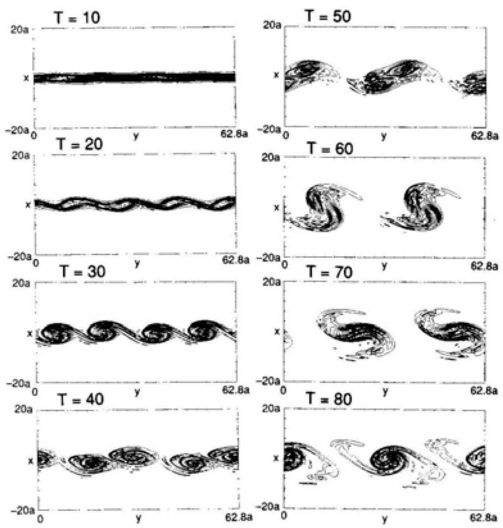

FIG. 5. Contour lines of the z component of the vorticity at eight different times from $T=10$ to $T=80$. In all panels the contour lines are plotted for negative vorticity (counterclockwise rotation).

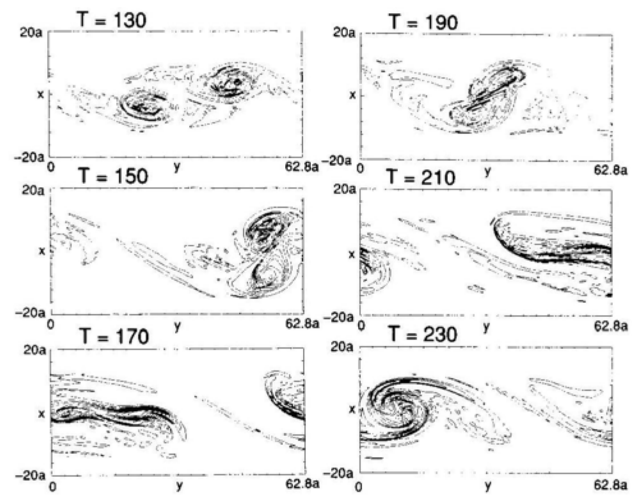

FIG. 6. Contour lines of the z component of the vorticity at six different times from $T=130$ to $T=230$. In all panels the contour lines are plotted for negative vorticity (counterclockwise rotation).

There is no initial shear of the magnetic field

From Miura.

The possible model for filamentary ELMs

The fluctuations are possibly Gaussian with rare extreme events. A strong fluctuation leads the system deep in the nonlinear stage of a KH instability, where the linear analysis (dispersion relation) is irelevant. The possible stabilization is governed by reaching a structure form, an extremum of the system's action.

We note the possible existence of a synergy: filament of vorticity are synergetic with filaments of current density.

- The isloated KH event triggers vortex nucleation
  - double spiral and effective radial constriction of the vorticity (experiments)
  - stretching of ω, parallel variation of the parallel current (conservation of ion polarization current)
  - stabilization of the annular vortex reaching the condition of a structure (field theory)
- start of a periodic modulation of density out of high ω centers (drop on ceil)
- baroclinic terms couple the density gradient with the gradient of perturbed B
- the current filamentation is enhanced by the z-forcing
- the local helical lines induce *swirl* and stabilize the vortex

The current and the vorticity have coincident maxima.

KH : There is a double spiral that is generated

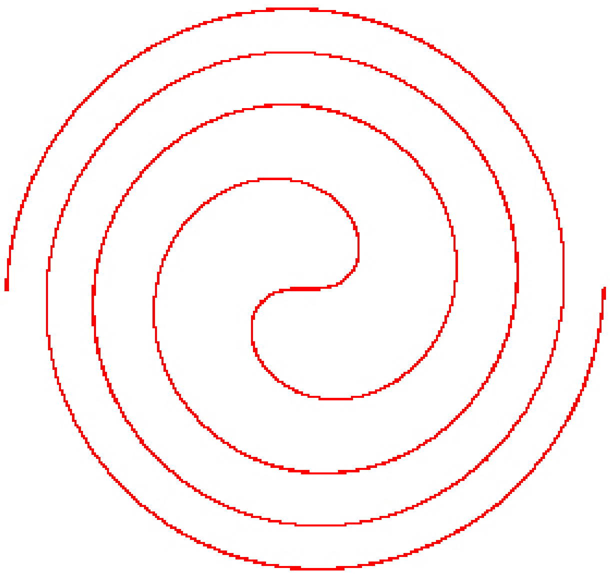

This is the Fremat Spiral

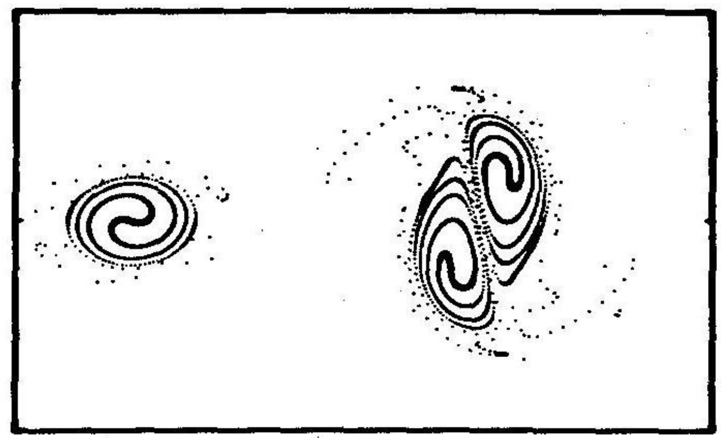

Moon Weidman
Local Vortex Pairing
PF31 (1988) 3804

FIG. 3. Secondary instability of the vortices when the shear layer is forced by mode $k_0/3$ with relative phase $\theta = -\pi/3$ [cf. Eq. (3)].

This is obtained from numerical simulations.

Vortex nucleation in strongly sheared velocity layers

Vortex nucleation is a process that appears when the vorticity goes beyond a certain level. It is then more convenient for the system (fluid or plasma) to generate vortices which concentrate the vorticity than to keep it distributed over a volume.

- superfluids
- protoplanetary disks
- Bose-Einstein condensates
- planetary atmosphere

There are two consequences of generating vortices: (1) the vorticity is transported and depleted into the smaller velocity part of the sheared layer (which means saturation of the poloidal rotation); (2) the sheared layer is destroyed and filaments replaces the layer, suppressing its property of transport barrier.

Let's see what happens to others.